RevMexAA (Serie de Conferencias), **5**, 9–15 (1996)

WINDS OF MASSIVE, MAIN SEQUENCE CLOSE BINARIES

R. H. Koch[1], I. Pachoulakis[1], R. J. Pfeiffer[2], and D. J. Stickland[3]

RESUMEN

Hemos emprendido un estudio sistemático de la geometría, estructura e interacciones de los vientos estelares de binarias cerradas de gran masa, que se ponen de manifiesto en las líneas de resonancia de N V, Si IV y C IV presentes en los espectros *IUE*. Solamente se analizan binarias para las cuales las curvas de luz contaminadas por vientos indican flujos conspicuos. Esta contribución resume nuestros resultados para HD 159176, Y Cyg y CW Cep surgidos de un análisis en dos pasos:
(a) Una versión modificada del programa *SEI* es empleada para calcular modelos de perfiles de líneas compuestos con vientos, en estado estacionario, para las líneas de viento observadas. Los residuos (modelado − observado) para las líneas de viento contienen evidencia de eclipses fotosféricos y de vientos así como de interacción de los vientos.
(b) Estos residuos son subsecuentemente modelados con un programa de interacción de vientos en binarias con el propósito de discernir las contribuciones de las interacciones individuales y buscar frentes de choque originados en la colisión de vientos.

La iteración entre estos dos pasos asegura la compatibilidad de los dos juegos de parámetros. Como resultado, se determinan consistentemente los parámetros que describen los vientos individuales, incrementos de densidad y choques.

ABSTRACT

We have undertaken a systematic study of the geometry, structure, and interactions of the stellar winds of massive, close binaries as evidenced by the N V, Si IV and C IV UV resonance lines in *IUE* spectra. Only binaries for which wind-contaminated light curves indicate conspicuous flows are analyzed. This contribution summarizes our results for HD 159176, Y Cyg, and CW Cep that have emerged from a two-step analysis:
(a) A modified version of the *SEI* code is employed to calculate steady-state, composite-wind model line profiles for observed wind lines. The (modeled − observed) wind-line residuals contain evidence for photospheric and wind eclipses and for wind interactions.
(b) These residuals are subsequently modeled by a binary wind interaction code for the purposes of disentangling the contributions from the individual interactions and for searching for colliding wind shock fronts.

Iteration between these two steps ensures compatibility of the two parameter sets. As a result, the parameters describing the individual winds, density enhancements, and shocks are determined consistently.

Key words: **BINARIES: CLOSE — LINE: PROFILES — STARS: EARLY-TYPE — STARS: MASS LOSS**

[1]University of Pennsylvania, USA.

[2]Trenton State College, USA.

[3]Rutherford Appleton Laboratory, USA.

1. INTRODUCTION

Our continuing program observing massive, close binaries with the *International Ultraviolet Explorer* (*IUE*) has a two-fold objective: to derive accurate fundamental stellar and orbital parameters, and to provide detailed understandings of the structure and interaction of the winds of these binaries. During an observing run, the archival images of a given target are supplemented by well-exposed, high resolution spectra, so that the Keplerian phase coverage is sufficiently dense for our objectives.

In a separate sequence of papers published in *The Observatory*, the *IUE* dataset for each binary is subjected to a cross-correlation technique which yields highly precise orbital elements. Coupled to light curve solutions which determine orbital inclinations and normalized stellar radii, the spectroscopic results give the absolute dimensions and geometry of a system. Section 2 familiarizes the reader with the three binaries of the present study, and Section 3 discusses the information content of wind-contaminated light curves. Section 4 presents our line of attack which develops the wind-related information from the available *IUE* datasets and displays some results. This involves a number of iterations between two steps: one that postulates a steady-state binary wind derived from modeling prominent wind lines in the spectra, and a second which examines the validity of such an understanding by modeling the residuals to those fits. After establishing consistency between the results of the two steps, the second-order residuals are examined in order to locate density enhancements or shocks. Finally, Section 5 summarizes our results for the three close binaries.

2. THE STELLAR SAMPLE

Sample orbital and stellar parameters for the three hot binaries in this study appear in Table 1. For the non-eclipsing HD 159176 the last three entries of Table 1 are enclosed within curly brackets to reflect the imprecision of those entries. The relative stellar parameters and normalized geometries of these binaries are comparable: the stars of each binary have approximately equal temperatures and luminosities, and their radii are $\approx a/4$. As a result, the kinetic energies of the individual winds and the interaction effects between them are expected to increase as spectral types become earlier.

TABLE 1

THE STELLAR SAMPLE

Binary	Spectral Class	$a\sin i(\mathrm{R}_\odot)$	i(°)	$R_{1,2}(\mathrm{R}_\odot)$	$M_{1,2}(\mathrm{M}_\odot)$
HD 159176	O6 V + O7 V	28.85	{50}	{9.8 , 9.3}	{32 , 32}
Y Cyg	O9.8 V + O9.8 V	28.3	85.5	6.0 , 6.0	16.7 , 16.7
CW Cep	B0.5 V + B0.5 V	23.8	82.5	5.64 , 5.14	12.9 , 11.9

3. EVIDENCE FOR SUPRA-PHOTOSPHERIC GAS IN UV LIGHT CURVES

Direct evidence for (or against) the existence of winds in binaries can be derived from the fact that winds are more extended than the photospheres from which they originate. At wind-line wavelengths the individual components should appear larger than at continuum bandpasses. To examine this assertion we derive light curves in bandpasses carefully placed across *IUE* spectra, as in Pfeiffer et al. (1994) and Pachoulakis et al. (1996).

The light curves which appear in the left column of panels of Figure 1 are derived by integrating dereddened line-blanketed continuum flux over the bandpasses indicated atop each panel. As a result, these light curves are not contaminated by wind activity. In the case of HD 159176 the visible and UV photometry of Thomas & Pachoulakis (1995) implies non-eclipsing photospheric disks (Pachoulakis 1996), but the proximity of the component stars results in ellipsoidal variability with an amplitude $\approx 0.07^m$ in the UV. On the other hand, the UV light curves for Y Cyg and CW Cep clearly show photospheric eclipses and are consistent with the concept of well-separated stars as is conveyed by the visible-band light curve solutions (e.g., Magalashvili & Kumsishvili 1959 and Clausen & Gimenez 1991, respectively).

Inspection of the images shows that C IV is the dominant wind feature for HD 159176 and Y Cyg whereas Si IV is more conspicuous in the spectra of CW Cep. Each light curve in the right column of Figure 1 is derived from the narrowest bandpass which contains the wind line profile. For example, a wind light curve for

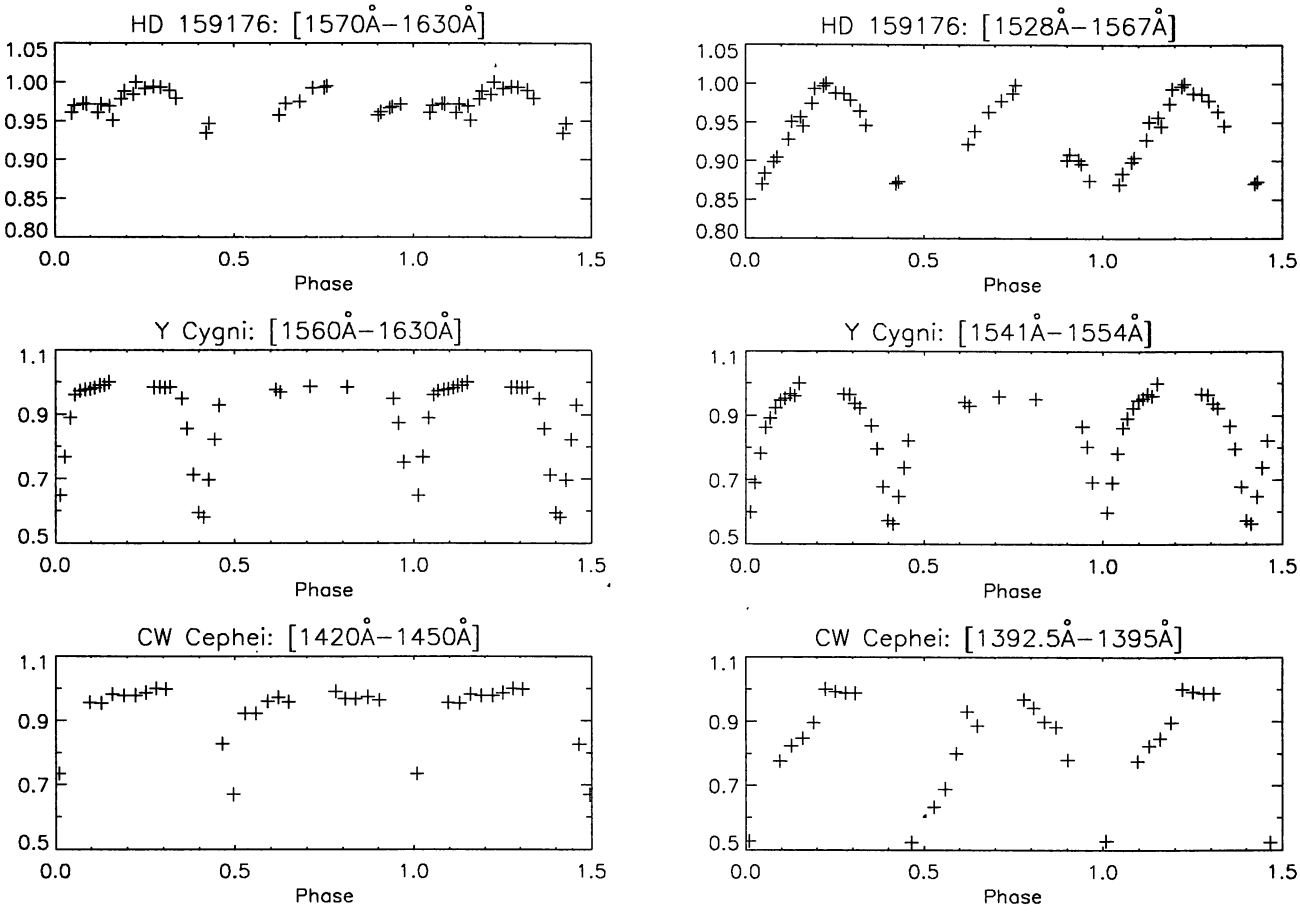

Fig. 1. Panels in left column: light curves derived from line blanketed continuum over the indicated bandpasses. Panels in right column: wind-affected light curves derived from bandpasses which contain a prominent wind line (the C IV feature for HD 159176 and Y Cyg, and the 1394Å Si IV feature for CW Cep).

HD 159176 is derived by integrating all dereddened flux between 1528Å and 1568Å and includes flux in emission as well as in absorption. Because of a reseau in the Si IV 1403Å wind-line, only the Si IV 1394Å feature is utilized for the case of CW Cep.

These wind-affected light curves are morphologically different from their continuum counterparts. For Y Cyg and for CW Cep, they show more continuous variability outside the photospheric eclipse intervals, implying larger-than-photospheric emitting surfaces and/or ellipsoidal variability that is more extreme than photospheric. The C IV wind light curve for HD 159176 is appreciably deeper than its photospheric counterpart and also implies extended and eclipsing winds (Pachoulakis 1996).

4. MODELING THE STRUCTURE AND INTERACTION OF HOT BINARY WINDS

The following two subsections summarize our two-step approach to modeling a sequence of phase-dependent wind-line profiles. A best-fit, based on our personal judgment, results from a number of iterations between the two steps and leads to a steady-state composite wind for a given binary. In addition, possibly transient features such as clouds and/or shocks are identified in the circumstellar wind volume.

4.1. Step A: Modeling the Wind Line Profiles

For each binary, the observed wind lines are modeled based on a variant of the *SEI* code of Lamers et al. (1987). That code, originally developed to model spherically-symmetric winds from single, non-rotating stars,

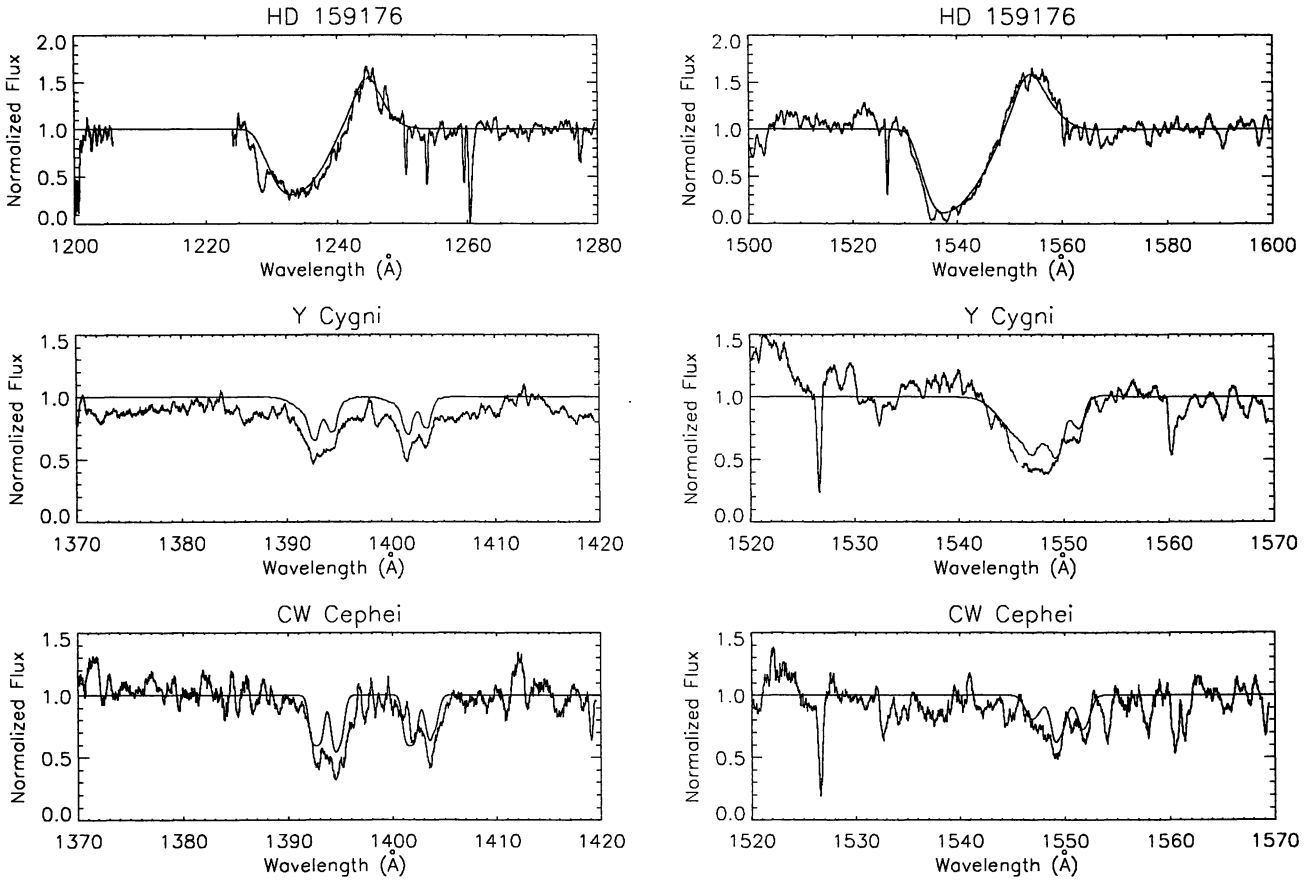

Fig. 2. Fits to observed wind lines at phases nearest quadrature; Top two panels: N IV and C IV features for HD 159176; Middle two panels: Si IV and C IV features for Y Cyg; Bottom two panels: Si IV and C IV features for CW Cep. All fits are shown for zero line-blanketing.

has been modified in order to accommodate orbital behavior and photospheric eclipses. For a particular wind line, the *SEI* code employs a β-type velocity law and a user-definable radial dependence for the optical depth. At any radius in the wind, turbulence may be introduced by a Gaussian distribution of wind speeds which is centered at the speed expected at that radius.

In the *Binary–SEI* (*BSEI*) approach an observed wind-line profile is modeled as a function of phase as follows. Initially a single *SEI* parameter set for each star generates one model line profile for that star. The two model profiles (one per star) are then combined in a manner consistent with the stellar light ratio determined from the photometric solution, with the radial velocity solution, and with the occurrence of photospheric eclipses. The procedure followed and its application to Y Cyg are detailed in Pfeiffer et al. (1994). The product of these calculations is a sequence of *BSEI* composite line profiles with phase-dependent morphology and these represent a first-order approximation to the steady-state winds from the binary.

Figure 2 presents *BSEI* fits for HD 159176 (the N V and C IV lines) and for Y Cyg and CW Cep (the Si IV and C IV lines) at phases nearest quadrature. Figure 3 collects selected wind parameters for each of the six stars in our binary sample. These have been calculated from the *BSEI* best-fits and appear to be monotonic functions of mass and, for this selection of stars, of luminosity. The stars of each binary are very similar to each other and this accounts for the nearly paired symbols in Figure 3. Although our stellar sample was not analyzed in either increasing or decreasing order of stellar mass, the very small scatter in those panels agrees with a consistent treatment of the images. Naturally, more systems must be studied before such a seemingly small scatter can be accepted as characteristic of hot, main-sequence double stars in general. Finally, the mass-loss rates quoted per star are reasonably consistent with those of other authors for comparable single stars.

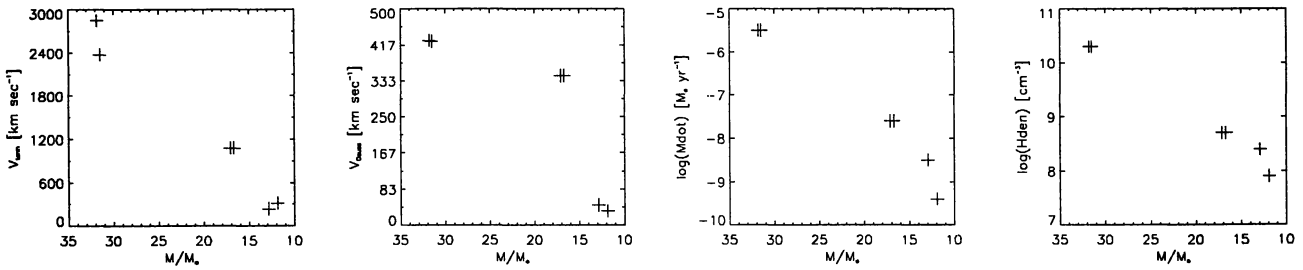

Fig. 3. Derived from the *BSEI* best-fit values for each of the 6 stars, the following parameters are plotted from left to right: the terminal wind speed, the half-width of the Gaussian turbulence velocity profile, the mass loss rate, and the hydrogen particle density at the interface between the two winds.

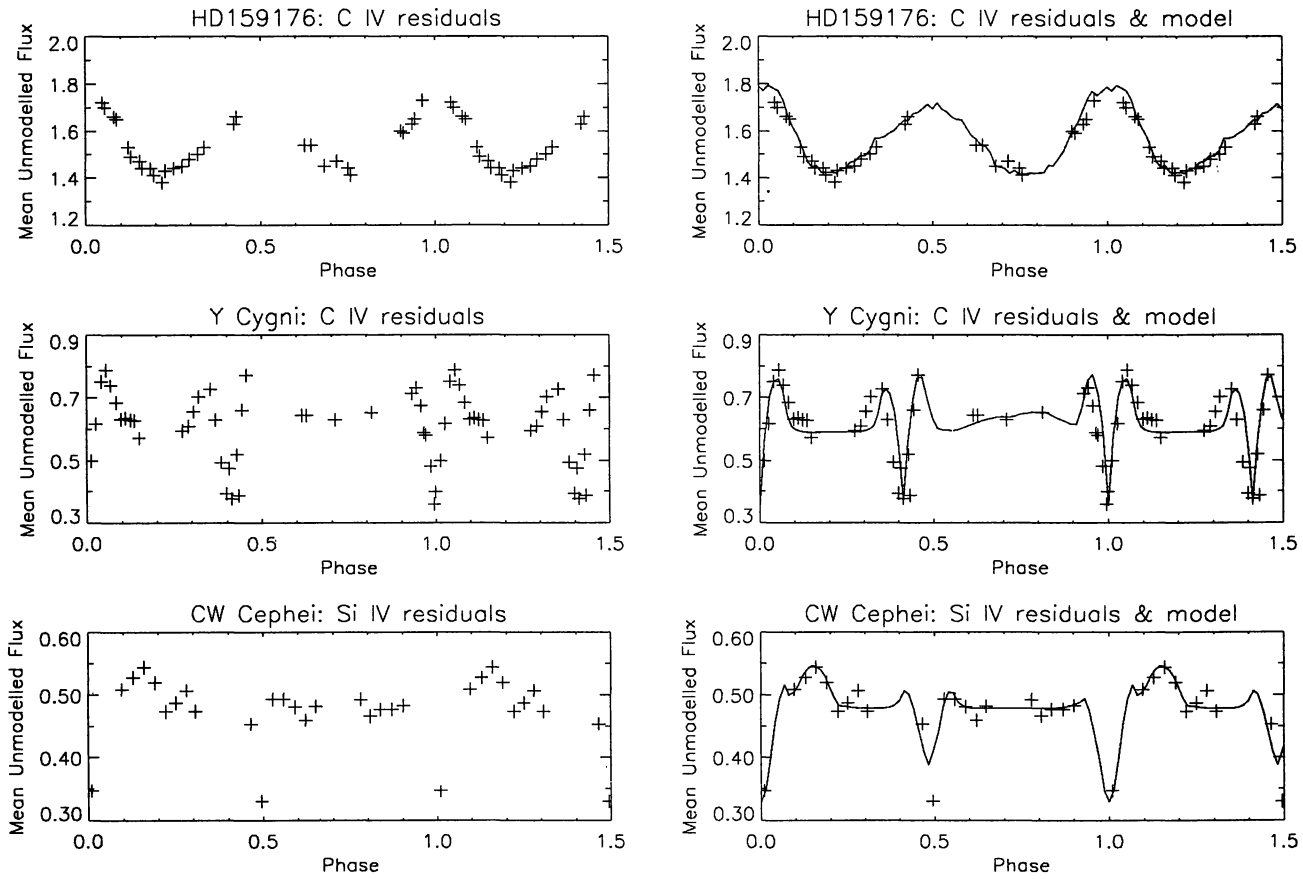

Fig. 4. For the dominant wind line of each binary, each panel on the left plots the unmodeled (i.e., *BSEI*–observed) residuals, averaged over the corresponding bandpass as shown in Figure 1 for that wind line. The corresponding panel on the right overplots the *BWI* model to those residuals. Unity on the ordinate scale is 10^{-10} ergs s^{-1} cm^{-2} $Å^{-1}$.

4.2. Step B: Modeling the Binary Wind-Interaction Effects

BSEI alone is incapable of yielding an accurate and complete fit to a wind profile for a binary system. This is because it does not account for the radiative transfer processes through both winds, the presence of wind enhancements observed at assorted aspects, and the effects of eclipses by the component stars. The evidence

for this statement appears in the left-hand panels of Figure 4, which show the unmodeled (*BSEI*−observed) residuals averaged over the corresponding bandpasses (cf., Figure 1) for each of the three binaries. The remaining wind lines, not illustrated here, show similar phase-dependent plots.

The orderly patterns of these unmodeled residuals justify our approach of employing *BSEI* to calculate a steady-state binary wind for a system. An alternative approach would entail calculating *BSEI* wind-line fits on an individual basis so as to null the residuals in Figure 4. In that case, however, the strong phase-dependence of the residuals apparent in Figure 4 would be diffused in the extended parameter space of *BSEI*. Similarly, information regarding temporal variations in the wind (such as those caused by DACs, shocks or clouds) would also be lost.

Our approach, on the other hand, utilizes *BSEI* as a means to a first-order approximation to the individual stellar winds. Then a second-order understanding follows from employing a Binary Wind Interaction (*BWI*) code which partitions the unmodeled residuals into the contributions of the individual wind-interaction effects i.e., winds against photospheres and winds against winds. The winds may include density enhancements which we call "clouds".

If the analysis be confined to the step A, the use of *BSEI* alone usually leads to an over-fit of the profile which, in turn, yields optical depths and extents for the winds that are too large. Practice has shown that *BSEI* and *BWI* must be applied iteratively in order to converge to a consistent fit. Accounting for wind-interaction effects allows substantial insight into the binary wind structure and offers more accurate photospheric profiles, wind optical depths and wind extents. In addition wind inhomogeneities can be located in the circumstellar volume.

An examination of the phase pattern of the unmodeled residuals is very informative and indicates inadequacies of a *BSEI* fit: unmodeled residuals above the level given by the line-blanketing (z) value at the conjunctions suggest an inhomogeneity eclipsing the photospheres and the winds, the former usually being the dominant effect; unmodeled residuals lower than required by the z-value at conjunctions indicate a source of emission in addition to that accounted for by *BSEI*, such as thermalization of wind kinetic energy in a shock front. That emission will be modulated mainly by eclipsing effects caused by the stars, with local maxima at quadratures and local minima at conjunctions.

For an eclipsing binary, the unmodeled residuals undergo a decrease at the conjunctions, mimicking the photospheric light curve of the system. This is due to the decrease in the total line blanketing in the spectrum. An increase in unmodeled absorption at phases just prior to first contact and immediately following last contact arises from the winds attenuating photospheric and wind fluxes. The amplitudes of these effects in both eclipses must be consistent with the wind optical depths of the *BSEI* fit.

In the first iteration between Steps A and B the individual wind optical depths, brightnesses, and extents are initial input to *BWI* based on the *BSEI* model from Step A. The results of such a fit then indicate possible inconsistencies of the *BSEI* fit, such as improper setting of the continuum level for the adopted value of z, an incorrect decrease in z at eclipses, and an improper modulation of the absorption near conjunctions.

Tactically, our approach has been conservative: we try to represent the unmodeled residuals first by the wind-wind and wind-photosphere attenuations. That aim having been satisfied, any systematic residuals still unmodeled are represented by wind inhomogeneities. Within the larger circumstellar volume, these are conceived of either as detached and bounded density enhancements (i.e., "clouds") at specific locations or as continuous enhancement fronts extending across the entire binary volume. Typically, the former evidence themselves as phase-bounded asymmetries in the unmodeled residuals curve beyond those imposed by an eccentric orbit. The latter, on the other hand, appear as phase-continuous modulations.

For each binary the results of iterating *BSEI* and *BWI* appear as the curves in the right-hand panels of Figure 4 and contain the signatures of the wind enhancements displayed in Figure 5. For HD 159176 the modulation of the *BSEI*-unmodeled residuals is dominated by the contribution of an extended wind enhancement located at the interface of the two winds (the fine structure of the continuous curve in the panel for HD 159176 is a computational artifact). A bounded "cloud" trailing Star 1 in the wind of Y Cyg raises the absorption level between phases 0.42 and 0.52 as well as near and following second quadrature. Finally, for CW Cep the local maximum of the unmodeled residuals at phase 0.15 can be accounted for by the "cloud" trailing Star 2.

5. CONCLUSIONS: COLLIDING WINDS

Obviously, it is only at the very end of our iterative procedure that any evidence for colliding winds can be adduced. Because the individual stars in each of the binaries presented herein are very similar to each other, wind interaction effects should be confined close to a layer midway between the stars and perpendicular to their

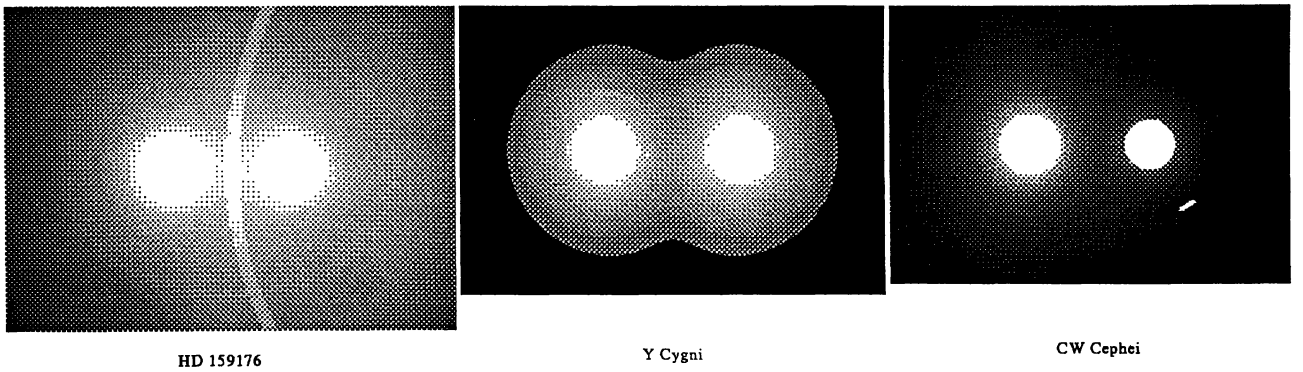

Fig. 5. A schematic, pole-on view of each binary at wind-line wavelengths, where the sense of rotation is in the counter-clockwise direction. Each panel shows the photospheric disks embedded in a halo representing the binary wind, and also the currently modeled shock for HD 159176 and the "clouds" for Y Cyg and for CW Cep.

line of centers. However, the outer wind layers of Y Cyg and CW Cep seem too thin to form an interaction region with a contribution above the S/N ratio of the *IUE* spectrometer. It is also possible that our treatment in its present formulation is unable to recover weak shock fronts. On the other hand, the individual winds of HD 159176 are sufficiently energetic to interact and give rise to an interface shock with a geometry and location indicated by the wind enhancement in Figure 5.

It is not presently clear whether the "clouds" of Y Cyg or CW Cep are expressions of wind variability (e.g., DACs). On the one hand, the *IUE* images that are useful to our approach were secured in the span of two consecutive Keplerian cycles (approximately 6 days). Because Y Cyg and CW Cep are eclipsing binaries and the "clouds" are positioned near zero stellar latitude, these "clouds" are visible for only fractions of each cycle. It is, therefore, possible that the *IUE* image set for each binary carries information that is really a snapshot of an evolving structure.

On the other hand, for the cases of Y Cyg and CW Cep we have only tried to recover clouds with pre-determined geometry, i.e., sections of a spherical shell. While we have been able to model the patterns displayed by the unmodeled residuals, it is possible that other structures of different geometries may also be able to account for the phase variability displayed by those patterns. However, in the absence of evidence pointing to the variability or evolution of these structures we have decided that the current approach is less likely to over-model the pattern of the residuals.

We conclude with the belief that comprehensive studies of main sequence binaries like the one presented herein serve two purposes: (1) they show conclusively how cool binaries may be and still develop wind interactions at low levels, and (2) they provide a foundation for the understanding of the significantly more extravagant interactions which are of interest in evolved systems.

REFERENCES

Clausen, J. V., & Gimenez, A. 1991, A&A, 241, 98
Lamers, H. J. G. L. M., Cerruti-Sola, M., & Perinoto, M. 1987, ApJ, 314, 726
Magalashvili, N. L., & Kumsishvili, Ya. I. 1959, Bull. Abastumani Obs., 24, 13
Pachoulakis, I. 1996, MNRAS, 280, 153
Pachoulakis, I., Pfeiffer, R. J., Koch, R. H., & Stickland, D. J. 1996, The Observatory, 116, 89
Pfeiffer, R. J., Pachoulakis, I., Koch, R. H., & Stickland, D. J. 1994, The Observatory, 114, 297
Thomas, J. C., & Pachoulakis, I. 1995, IBVS, 4115